

TurboSAT: Gradient-Guided Boolean Satisfiability Accelerated on GPU-CPU Hybrid System

Steve Dai*, Cunxi Yu, Kalyan Krishnamani, Brucek Khailany

NVIDIA

*sdai@nvidia.com

Abstract—While accelerated computing has transformed many domains of computing, its impact on logical reasoning, specifically Boolean satisfiability (SAT), remains limited. State-of-the-art SAT solvers rely heavily on inherently sequential conflict-driven search algorithms that offer powerful heuristics but limit the amount of parallelism that could otherwise enable significantly more scalable SAT solving. Inspired by neural network training, we formulate the SAT problem as a binarized matrix-matrix multiplication layer that could be optimized using a differentiable objective function. Enabled by this encoding, we combine the strengths of parallel differentiable optimization and sequential search to accelerate SAT on a hybrid GPU-CPU system. In this system, the GPUs leverage parallel differentiable solving to rapidly evaluate SAT clauses and use gradients to stochastically explore the solution space and optimize variable assignments. Promising partial assignments generated by the GPUs are post-processed on many CPU threads which exploit conflict-driven sequential search to further traverse the solution subspaces and identify complete assignments. Prototyping the hybrid solver on an NVIDIA DGX GB200 node, our solver achieves runtime speedups up to over 200x when compared to a state-of-the-art CPU-based solver on public satisfiable benchmark problems from the SAT Competition.

I. INTRODUCTION

Boolean satisfiability (SAT) is a fundamental NP-complete problem of determining whether there exists an assignment of truth values to variables that satisfies a given Boolean formula [1]. As shown in Figure 1, a SAT formula is typically expressed in Conjunctive Normal Form (CNF) consisting of a conjunction of clauses where each clause is a disjunction of literals. Each literal represents a variable or its negation, and each variable can be assigned a truth value of either 1 (True) or 0 (False). A SAT problem is considered satisfiable if there exists at least one assignment of the variables such that every clause contains at least one true literal. Otherwise, the problem is deemed unsatisfiable (UNSAT). Figure 1 shows a satisfiable problem along with a satisfying assignment. As a cornerstone of modern logical reasoning, SAT serves as an integral component of computer-aided design (CAD) and plays a critical role in challenging combinatorial problems.

Modern SAT solvers typically employ a systematic search algorithm known as Conflict-Driven Clause Learning (CDCL) which explores variable assignments through an iterative process of decision, propagation, conflict learning, and backtracking [2]. CDCL’s effectiveness stems from its ability to prune future search spaces using learned conflict clauses and to backtrack non-chronologically to specific decision level responsible for a conflict, skipping redundant exploration. Depending on the particular solver, CDCL is often complemented with various

SAT problem	CNF Clauses	Satisfying Assignment
p cnf 4 5		
1 2 0	1. $x_1 \vee x_2$	$x_1 = 0$
3 4 0	2. $x_3 \vee x_4$	$x_2 = 1$
-1 -3 0	3. $x'_1 \vee x'_3$	$x_3 = 0$
-1 -2 -4 0	4. $x'_1 \vee x'_2 \vee x'_4$	$x_4 = 1$
1 4 0	5. $x_1 \vee x_4$	

Fig. 1. SAT problem in CNF with 4 variables and 5 clauses – The problem is satisfiable because each clause has at least one satisfied (bold) literal.

specialized heuristics to further improve efficiency. For example, MiniSat introduces phase saving to remember previously assigned values [3]. CaDiCaL offers clause subsumption to remove clauses containing redundant information [4]. CDCL-based solvers are often integrated within CAD tools to tackle industrial-grade problems in formal verification, automatic test generation, and other chip design tasks [5].

Despite its success, CDCL relies on an inherently sequential search algorithm, which limits the potential for parallelism. Prior efforts to parallelize SAT solving based on CDCL include performing divide-and-conquer on the decision tree [6] or employing a portfolio of solvers with different policies and heuristics [7]. In addition, several SAT solvers have been developed to leverage the parallel processing power of GPUs. For example, ParaFROST accelerates inprocessing on GPU with parallel variable elimination, eager redundancy elimination, and a GPU-based garbage collector [8]. Fujii and Fujimoto parallelizes Boolean Constraint Propagation (BCP) on GPU with clause partitioning, allowing different groups of clauses to be processed in parallel during the propagation phase [9].

Driven by the demands of artificial intelligence and high-performance computing, heterogeneous architectures that tightly integrate GPUs, CPUs, memory, and interconnects are emerging as the go-to systems for accelerated computing. NVIDIA’s Grace Blackwell Superchip exemplifies this trend by combining the Blackwell GPU with the many-core Grace CPU through a unified memory model and high-speed NVLink interconnects [10]. Notably, GPUs are optimized for large-scale parallel matrix operations typical in deep learning (DL) workloads, while many-core CPUs excel at executing an abundance of sequential tasks simultaneously across many threads. We henceforth refer to a GPU-CPU system as a hybrid system in the rest of the paper. These hybrid systems present opportunity to re-imagine SAT solving beyond traditional CDCL, combining the exploratory power of parallel optimization on GPU and the exploitation power of sequential search on CPU.

To address these opportunities, we present a novel SAT algorithm that harnesses the GPU-CPU synergy to efficiently tackle SAT solving in two distinct phases: GPU-enabled parallel differentiable optimization and CPU-friendly conflict driven search. This algorithm dramatically accelerates SAT solving using an exploration-exploitation approach. Specifically, our key contributions are as follows:

- *Differentiable Formulation*: We formulate the SAT problem as a binary matrix-matrix multiplication layer paired with a differentiable objective function for SAT solving. This formulation enables gradient-guided optimization of variable assignments to maximize satisfiability.
- *Massively Parallel Exploration*: We utilize differentiable solving on the GPU to iteratively evaluate SAT clauses and optimize variable assignments with massive parallelism. This allows the solver to rapidly explore the large solution space and quickly identify promising solution subspaces.
- *Conflict-Driven Exploitation*: We post-process promising partial assignments identified by the GPU with many parallel CPU threads. Each thread exploits conflict-driven learning and sequential search to further traverse solution subspaces and identify complete assignments efficiently.
- *Implementation*: We prototype our solver on a DGX GB200 GPU-CPU system using one GPU instance and 100 CPU threads. On satisfiable benchmarks from the 2024 SAT Competition, our hybrid solver achieves runtime speedup up to over 200x over a state-of-the-art CPU-only solver.

II. RELATED WORK

Mirroring the broader trend of machine learning for CAD, neural networks have emerged as potential candidates for augmenting or even replacing traditional SAT algorithms [11]. In this context, recent work has introduced both supervised and unsupervised learning techniques as new paradigms for SAT solving. These techniques leverage specialized neural network architectures to represent SAT instances by encoding variables, clauses, and their constraints into continuous embeddings.

A. Supervised Learning for SAT

Supervised learning techniques for SAT solving involve training neural networks on labeled SAT instances to predict solutions or guide solver heuristics. NeuroSAT proposes an end-to-end approach that leverages Graph Neural Network models to encode the relationship among the variables and treat SAT solving as a binary classification problem [12]. Satisfying assignments are decoded from the learned variable embeddings. SATFormer extends this paradigm with hierarchical Transformer-based architectures to model clause correlations, enabling both satisfiability prediction and identification of unsatisfiable sub-problems, also known as UNSAT cores [13]. While these end-to-end methods demonstrate some promise, they require large labeled datasets and remain less efficient and accurate than state-of-the-art CDCL solvers in practice. Other supervised learning based approaches focus on enhancing specific heuristics used by traditional SAT solvers. For example, NeuroCore predicts variables involved in the UNSAT core to influence variable branching decisions [14]. NeuroBack

predicts values of variables that tend to appear in satisfying assignments [15]. Despite their emphasis on specific heuristics, these techniques depend on extensive training data and can struggle to generalize to unseen problem distributions.

B. Unsupervised Learning for SAT

Unsupervised learning techniques for SAT solving eliminate the need for labeled data or pre-solved instances by reformulating SAT problems into optimization tasks that directly learn the SAT solutions without prior model training. Fourier-SAT transforms SAT solving into continuous optimization via Walsh-Fourier expansions, converting Boolean constraints into multilinear polynomials and guiding search through gradient-driven local improvements instead of combinatorial enumeration [16], [17]. However, this method provides incremental improvement over existing methods. DiffSAT introduces a differentiable MaxSAT layer that transforms SAT solving into a gradient-based minimization task [18]. It initializes assignments via semidefinite relaxation and iteratively refines them using a clause-violation loss function. However, the algorithm's single-variable update strategy limits parallelism, hindering time to convergence and scalability on GPU architectures.

III. DIFFERENTIABLE FORMULATION

Following the unsupervised learning approach, we propose a novel SAT-solving framework that combines matrix-based problem encoding inspired by GPU4SAT [19] with differentiable optimization. Unlike existing methods, our approach focuses on leveraging GPU-accelerated General Matrix Multiplication (GEMM) to evaluate SAT problems with efficiency and massive parallelism, essentially transforming combinatorial search into a high-throughput optimization task. For the rest of this section, let's consider a SAT problem represented in the CNF format that contains V variables and C clauses. For convenience, we will illustrate our formulation using a small SAT problem with 4 variables ($V = 4$) and 5 clauses ($C = 5$) in Figure 2, same as the problem in Section I and Figure 1.

A. Binary Matrix Encoding

We encode the SAT problem into a matrix-matrix multiplication $R = PA$ in which the Problem Matrix $P \in \{0, 1\}^{C \times 2V}$ represents the clauses and literals and the Assignment Matrix $A \in \{0, 1\}^{2V \times N}$ represents the variable assignments. The Result Matrix $R \in \mathbb{Z}_{\geq 0}^{C \times N}$ indicates the satisfiability of each clause in the problem. N is the runtime parameter that denotes the number of SAT assignments that we attempt. This encoding allows for the parallel evaluation of all N assignments on all C clauses using GPU hardware.

1) *Problem Matrix*: We encode the SAT problem in CNF format into a Problem Matrix P with C rows and $2V$ columns. Each row represents a single clause, and each column represents a literal, meaning a single variable or its negation. We allow only 0's and 1's in the matrix, which requires allocating two separate columns in P for each variable in the SAT problem. In our encoding, a value of 1 in P indicates that the corresponding literal is present in the clause, while a 0 indicates that the corresponding literal is absent in the clause. As illustrated in

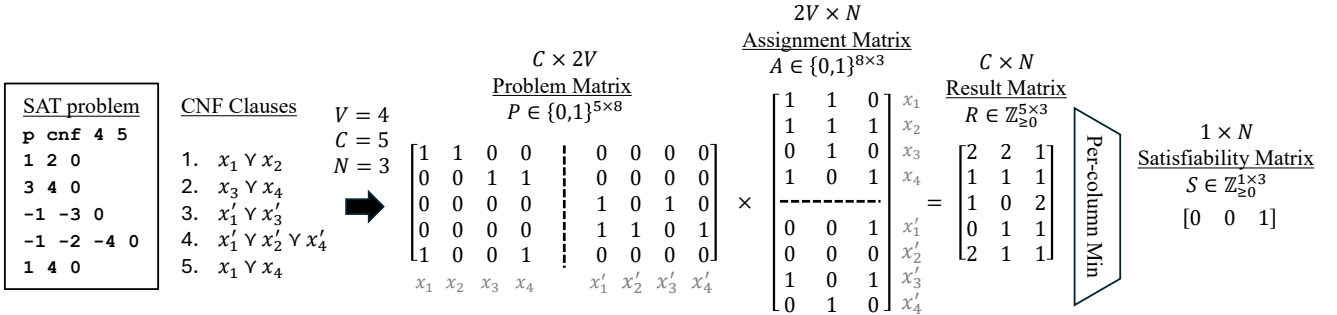


Fig. 2. **Binary matrix multiplication encoding for our differentiable SAT formulation** – Each row of the Problem Matrix encodes one corresponding CNF clause. Each column of the Assignment Matrix represents one candidate assignment being attempted. Each element in the Result Matrix indicates the number of literals that each candidate assignment satisfies in each clause. The Satisfiability Matrix indicates whether each assignment is satisfying all clauses.

Figure 2, the second clause maps to 1’s in the x_3 and x_4 columns in the second row of P . P is analogous to the input activation tensor in a DL layer.

2) *Assignment Matrix*: We encode the N assignments being attempted by the solver into an Assignment Matrix A with $2V$ rows and N columns, where N can be increased to attempt more assignments and explore a larger search space. In A , 0 indicates that the corresponding literal is assigned False, and 1 indicates that the corresponding literal is assigned True. In Figure 2, for example, the second assignment assigns x_1 , x_2 , and x_3 to True while assigning x_4 to False. We consider only complete assignments in A where every variable is assigned either True or False. Therefore, a literal always has an assignment which is opposite to that of its negated counterpart. For example, in the second assignment, because x_1 is True, x_1' must be False. Same goes for all other variables and assignments. A is analogous to the weight tensor in a DL layer.

3) *Result Matrix*: Multiplying the Problem Matrix P into the Assignment Matrix A produces the Result Matrix R with C rows and N columns. Each column represents the result of the corresponding assignment. Each row in an assignment denotes the number of literals in the corresponding clause that the assignment is able to satisfy (i.e., evaluate to True). In Figure 2, Row 3 Column 2 of the Result Matrix is 0 because the second assignment assigns neither x_1 nor x_3 of the third clause to False. On the other hand, Row 3 Column 3 of the Result Matrix is 2 because the third assignment assigns both x_1 and x_3 in the third clause to False, resulting in two literals that can be used to satisfy this clause. R is analogous to the output activation tensor in a DL layer.

4) *Satisfiability Matrix*: By computing the column-wise minimum of the Result Matrix R , we derive the Satisfiability Matrix $S \in \mathbb{Z}_{\geq 0}^{1 \times N}$. Each entry in S represents the minimum number of literals satisfied by the corresponding assignment in any clause and indicates the satisfiability of each assignment. If the per-column minimum is zero, the corresponding assignment is not able to satisfy all the clauses because there exist at least one clause in which the assignment fails to satisfy even a single literal. If the per-column minimum is nonzero, the corresponding assignment is able to satisfy all the clauses because the assignment satisfies at least one literal in every clause of the problem. If the maximum value of the Satisfiability Matrix S is nonzero, at least one out of the N assignments is a satisfying assignment, and the problem is satisfiable. However, if the

maximum value of S is zero, there is no satisfying assignments among those attempted, and the problem is indeterminate. Note that we can declare UNSAT only if all possible assignments have been exhausted. In this paper, we focus only on satisfying assignments, and leave UNSAT problems to future work.

B. Differentiable Solving

We leverage forward and backward passes to perform differentiable SAT solving based on our formulation in Section III-A. For convenience, we can interpret the matrix multiplication $R = PA$ defined in Section III-A as a Linear layer, where P serves as the non-trainable input activation tensor and A represents the trainable weight parameter tensor. The computation graph of the binarized matrix multiplication layer used for SAT solving is detailed in Figure 3. During differentiable optimization, the forward pass (illustrated by solid arrows) evaluates the current set of assignments on the SAT clauses by computing the following matrix multiplication.

$$R = PA \quad (1)$$

Subsequently, the backward pass (illustrated by dash arrows) computes the gradients in respect to the assignment $\partial \mathcal{L} / \partial A$ and updates the assignments A accordingly to maximize satisfiability. Here \mathcal{L} denotes the loss function that encodes satisfiability. Because the activation tensor is not trainable in a Linear layer, we can use the 0/1 Problem Matrix P directly as the input that is repeatedly passed into the matrix multiplication at each iteration. However, to enable proper flow of gradients in the backward pass, we use a real-valued matrix $A_{real} \in \mathbb{R}^{2V \times N}$ in place of the binary matrix A as the trainable weight tensor of the matrix multiplication under the hood. The binary Assignment Matrix A defined in Section III-A is simply the binarization of A_{real} based on this binarization function B .

$$A = B(A_{real}) = \text{clip}(\text{sign}(A_{real}), 0, 1) \quad (2)$$

The training objective for SAT solving aims to achieve satisfiability, meaning that the Satisfiability Matrix S contains at least one nonzero value. As a proxy, our differentiable objective function is formulated to maximize the sum of the Satisfiability Matrix S , giving the loss function \mathcal{L} as follows.

$$\mathcal{L} = - \sum_{i=1}^N S_i \quad (3)$$

However, S is in turn derived from the per-column minimums of the Result Matrix R , where the minimum function is not

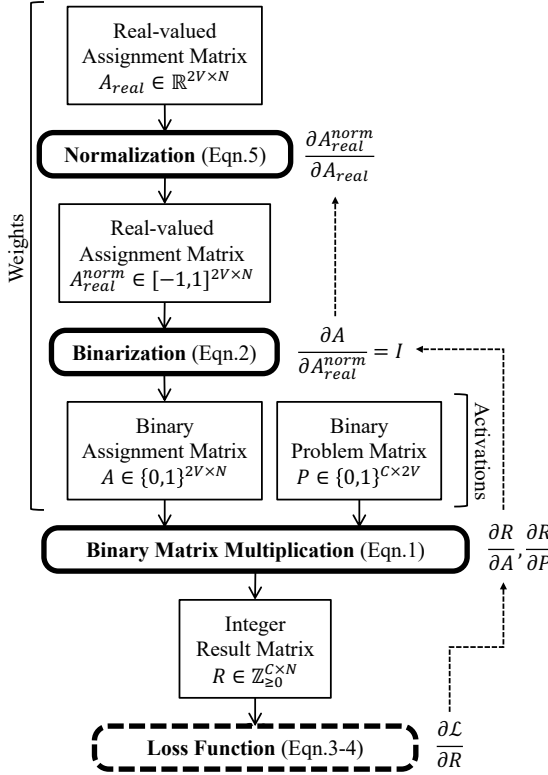


Fig. 3. **Computation graph of the binary matrix multiplication for SAT solving** – In the forward pass (solid arrows), the trainable weights are normalized and binarized prior to multiplication. In the backward pass (dash arrows), an identity function is used as a proxy for gradient propagation through the non-differentiable Binarization layer.

differentiable. Therefore, we use a differentiable smooth minimum function instead of a hard minimum on each column of R , denoted R_i , to facilitate gradient propagation. By applying the smooth minimum function, the Satisfiability Matrix S in the loss function \mathcal{L} is defined such that

$$S_i = \text{SmoothMin}(R_i) = \frac{\sum_{j=1}^C R_{ij} e^{-\tau R_{ij}}}{\sum_{j=1}^C e^{-\tau R_{ij}}} \quad (4)$$

where SmoothMin converges to a minimum function as τ approaches $+\infty$. For the Binarization Layer in Figure 3, we binarize the parameter tensor A using the $B(x)$ function in Equation 2 by clamping all positive values to 1 and all non-positive values to 0. Following the convention of quantization-aware training [20], we don't explicitly compute the gradients of the Binarization Layer, but use straight-through estimator (STE) instead to pass gradients as-is [21].

IV. GRADIENT-GUIDED HYBRID SOLVING

Building on the differentiable SAT formulation from Section III, we propose a hybrid solving architecture that synergistically combines GPU-driven differentiable optimization with CPU-based combinatorial search, leveraging the complementary strengths of a hybrid GPU-CPU system. On the GPU, gradient-guided optimization enables rapid exploration of the assignment space through massively parallel matrix operations to evaluate many assignment candidates simultaneously. On the CPU, CDCL refines promising candidates from the GPU using heuristic-guided conflict-driven search. Exploiting

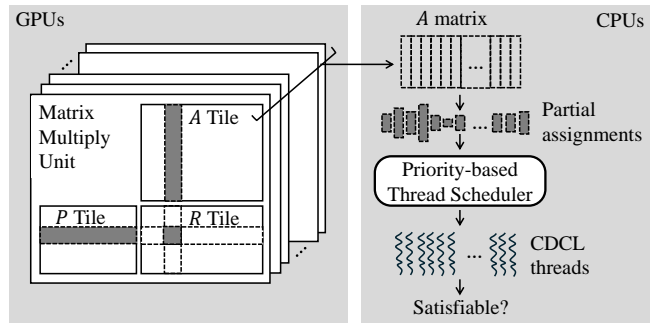


Fig. 4. **Hybrid SAT solving on GPU-CPU system** – GPUs perform differentiable optimization on matrix-multiply units. CPUs leverage CDCL search on many threads to determine complete satisfying assignments.

their respective computational advantages, the GPU focuses on broad, parallel exploration to identify high-likelihood subspaces, while the CPU specializes in precise, sequential refinement to resolve remaining conflicts in narrowed subspaces. This approach bridges the gap between gradient-based optimization and conflict-driven search techniques. The hybrid SAT solving system is shown in Figure 4.

A. Gradient-based Optimization on GPU

Based on the matrix encoding from Section III-A, we construct the Problem Matrix P by parsing each clause in the CNF of the problem, followed by initializing the N assignments in the real-valued Assignment Matrix A_{real} with random values from the standard normal distribution. This initialization ensures that binarizing A_{real} to A yields a balanced number of 0's and 1's, equivalent to assigning approximately half the variables to True and False, respectively. Once the problem is constructed in the form of our $R = PA$ layer, we iteratively optimize A_{real} , and in turn the binary assignments in A , by performing forward and backward passes as described in Section III-B.

For the optimization process, we use the AdamW optimizer with an initial learning rate of 10^{-1} and a final learning rate of 10^{-15} . We follow a stepwise decay schedule that reduces the learning rate by a factor of 10 every 30 iterations. This schedule enables aggressive early exploration (using high learning rate) followed by more careful refinement (using small learning rate), which can effectively reduce the number of remaining UNSAT clauses. We perform periodic restart by resetting the learning rate back to 10^{-1} after every 360 iterations. Our learning rate reset strategy helps navigate around previously best assignments (i.e., local minima) in a rugged optimization landscape and converge towards superior assignments. We apply these settings consistently on all experiments reported in Section V.

To further improve the efficiency of learning the best variable assignments, we perform per-variable normalization on the real-valued Assignment Matrix A_{real} to enable information sharing on a per-variable basis among all the attempted assignments. For row j in A_{real} , we compute the mean of the row and scale each element in the row by the mean as shown in Equation 5.

$$A_{real,ij}^{norm} = \frac{A_{real,ij}}{\frac{1}{N} \sum_{i=1}^N A_{real,ij}} \quad (5)$$

We append this normalization operation in front of the Binarization Layer, as shown in Figure 3. It is fully differentiable and able to propagate gradients in the standard fashion.

Lastly, we observe that our Problem Matrix P is highly sparse. Therefore, we encode P using the compressed sparse format, enabling highly efficient sparse matrix multiplications in both the forward and backward passes. This encoding results in dramatic reduction in memory usage and significant acceleration in differentiable optimization, helping scale our technique to very large problems.

B. CDCL-based Refinement on CPU

Once the optimization on the GPU converges, approximated by satisfying over 99% of the clauses in the problem, we extract the truth values of the k most confident variables from each candidate assignment, where k is 0.01% of the number of variables but at least 20. Confidence is quantified using the final gradient magnitudes of the variables as a proxy, where smaller absolute gradient values indicate variables who have higher confidence in their current assignments. The set of high-confidence variables (with minimal gradient magnitudes) along with their respective assignments are selected to initialize the CDCL solver, as shown in Figure 4.

On the CPU side, each thread receives a partial initialization from the GPU and executes a CDCL-based SAT solver instance from the partial initialization, leveraging conflict-driven learning to resolve the remaining variables. The partial initialization is meant to assist the CDCL solvers in deriving satisfying solutions in significantly less time than starting from scratch. The number of partially initialized parallel CDCL instances scales with the number of CPU threads available on the system, akin to a portfolio solver strategy. However, we distinguish from prior portfolio solvers by starting with confident partial assignments from GPU-driven gradient-based optimization instead of starting from scratch from random seeds and/or using different solver configurations. If the number of available CPU threads is insufficient to dispatch the entirety of the assignments in the Assignment Matrix A , we prioritize the assignments with higher number of satisfied clauses.

Anchoring just a small fraction of variables may seem insignificant at first sight; but it can dramatically improve solver efficiency in multiple aspects. Theoretically, assigning V^* variables prunes the search space exponentially by 2^{V^*} , which represents orders-of-magnitude reduction that effectively narrows the CDCL solver’s focus to high-likelihood subspaces [22]. Practically, these assignments trigger the BCP procedure which simplifies clauses by removing satisfied literals and deduces additional variable assignments through unit propagation. Industrial SAT instances, typically characterized by a small subset of variables influencing numerous clauses simultaneously, amplify the aforementioned benefits by enabling cascading simplification and conflict resolution opportunities [23]. Essentially, our approach transforms CDCL from under-informed search into targeted refinement, achieving efficiency gains atypical through random or heuristic initialization alone. Without gradient guidance, randomly initializing the same number or same subset of variables would provide minimal benefit to CDCL.

V. EXPERIMENTS

We prototype our hybrid solver on an NVIDIA DGX GB200 accelerated computing system instance equipped with four NVIDIA Blackwell B200 GPUs and two NVIDIA Grace CPUs each with 72 ARM Neoverse V2 cores [24]. Although there are four GPUs and 144 CPU cores, we limit our solver to use up to only two GPUs and 141 CPU threads. Our solver leverages the PySAT framework [25] for parsing input problems and interfacing with CDCL SAT solvers. Gradient-based optimization is executed on the GPU using PyTorch 2.2 [26], while CDCL-based refinement is run on the CPU with the CDCL solver CaDiCaL 1.9.5 [27]. Our setup mimics the system shown in Figure 4. To ensure fair comparison, we use the same CaDiCaL solver for our baseline experiments. CaDiCaL is a state-of-the art SAT solver used in industry and one of the top contenders in the SAT Competition. We evaluate runtime performance on all satisfiable benchmark problems from the 2024 SAT Competition [28].

In Table I, we first detail the runtime results of our hybrid solver on selected representative problems of various sizes and types and compare them to the results of the baseline solver CaDiCaL. We would like to point out that our solver is always at least as competitive as CaDiCaL, as we dedicate one thread to running CaDiCaL from scratch. For each benchmark, alongside basic problem statistics, we list the runtime in seconds for both CaDiCaL and our solver. Due to the hybrid nature of our solver, we report the total runtime (denoted `Total`), as well as the runtime spent in the gradient-guided optimization phase (denoted `Gradient`) and the CDCL-based refinement phase (denoted `CDCL`). To quantify the performance gain, we include the total speedup relative to CaDiCaL, as well as the speedup achieved during the CDCL refinement phase alone. Because our hybrid solver internally uses the same CaDiCaL solver as our baseline CaDiCaL, the latter speedup precisely reflects the benefit of initializing with gradient-guided partial assignments.

Benchmarks in Table I are sorted by their total speedup. Many problems achieving significant speedup have been omitted in Table I due to space constraints, but are included in the cumulative runtime performance plot in Figure 5. In Table I, benchmarks for which CaDiCaL times out after two hours are listed first. Compared to CaDiCaL, our solver achieves a total runtime speedup of 5.03x to 258.08x on the listed benchmarks. Considering CDCL alone, our partial initialization strategy observes a speedup from 5.94x to 1367.73x. Notably, our solver sees greater than 10x total speedup for benchmarks with up to more than 74,000 variables and 393,000 clauses. Our solver also solves many problems within 1000 seconds for which CaDiCaL times out even after two hours.

Specifically, our solver achieves greater than 100x speedup for the two `x9` benchmarks, solving them in seconds compared to more than 20 minutes spent by CaDiCaL. Our solver also achieves greater than 20x speedup for the `j3037` problem with a clause-to-variable ratio of 4.53, close to the critical 4.25 threshold where a problem tends to be hardest to solve [29]. Furthermore, we see a speedup of 26.31x on the `ex065_25` problem with 74,776 variables and 393,322 clauses, representing problems of non-trivial size. On the problems for which

TABLE I

SELECTED RUNTIME COMPARISON – TOTAL DENOTES THE TOTAL RUNTIME OF OUR SOLVER. GRADIENT DENOTES THE GRADIENT-GUIDED OPTIMIZATION PORTION. CDCL DENOTES THE CDCL PORTION. TIMEOUT IS 7200 SECONDS. SPEEDUP COMPARES OUR SOLVER AGAINST CADiCaL.

Benchmark	#Variables	#Clauses	Ratio	Runtime (seconds)			Speedup	
				CaDiCaL	Ours		CDCL	Total
					Gradient	CDCL		
pcmax-scheduling-m12-8049-55035-SAT	8048	55035	6.84	Timeout	5.19	30.76	35.95	Unknown Unknown
6g_6color_366_050_04	77328	8485566	109.73	Timeout	47.44	3.50	50.94	Unknown Unknown
002	4128	126564	30.66	Timeout	4.93	102.27	107.20	Unknown Unknown
pcmax-scheduling-m40-26287-324155-SAT	26286	324155	12.33	Timeout	7.52	99.86	107.38	Unknown Unknown
Folkman-185-19924337	17019	19874	1.17	Timeout	4.53	281.05	285.58	Unknown Unknown
mdp-32-11-sat	1038	5842	5.62	Timeout	9.18	659.29	668.47	Unknown Unknown
Break_20_72.xml	53844	270142	5.01	Timeout	9.28	956.74	966.02	Unknown Unknown
Nb13T165	1389990	5543200	3.98	Timeout	58.06	1251.36	1309.42	Unknown Unknown
fermat-931960058139995587	12257	69473	5.66	Timeout	6.86	2483.75	2490.61	Unknown Unknown
1-ET-512-K-96.sanitized	45616	2068700	45.35	Timeout	85.93	2435.51	2521.44	Unknown Unknown
apn-sbox5-cut3-symmbreak	21240	86081	4.05	Timeout	4.67	2913.15	2917.82	Unknown Unknown
x9-11053.sat.sanitized	550	4951	7.40	1244.63	3.91	0.91	4.82	1367.73x 258.08x
x9-12014.sat.sanitized	600	5405	9.01	1692.45	3.95	5.53	9.48	306.05x 178.50x
combined-crypto1-wff-seed-1-wffvars-450	1729	21718	12.56	176.26	4.59	1.24	5.83	142.15x 30.21x
j3037_9_rggt_b	18913	85707	4.53	396.37	4.82	10.11	14.93	39.21x 26.55x
ex065_25	74776	393322	5.26	1492.35	10.35	46.37	56.72	32.18x 26.31x
rbsat-v760c43649gyes3	760	43639	57.42	129.96	4.39	1.08	5.47	120.33x 23.75x
Circuit_multiplier22	1013	18793	18.55	233.56	5.31	7.42	12.73	31.48x 18.35x
004	4288	132576	30.92	1490.67	5.04	95.94	100.98	15.53x 14.76x
af-synthesis_stb_50_40_9_sat	15981	124882	7.81	740.29	5.75	48.07	53.82	15.40x 13.75x
noL-11-20.sanitized	1419	7841	5.52	82.25	3.91	5.04	8.95	16.32x 9.19x
preimage_80r_495m_160h_seed_379	56108	224206	3.99	216.86	6.61	36.52	43.13	5.94x 5.03x
All satisfiable problems	-	-	-	-	-	-	-	Average 27.30x

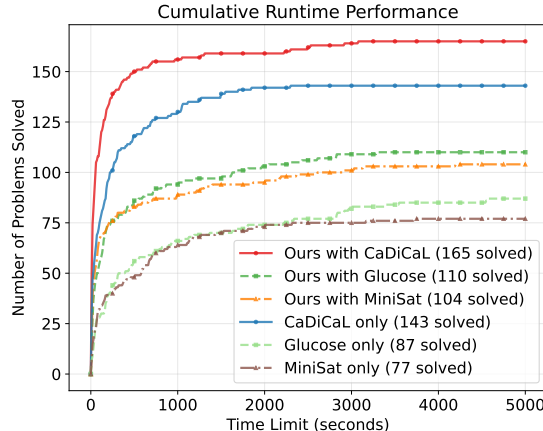


Fig. 5. Cumulative performance curve – Compares the number of solved problems for a given time limit between our solvers and baseline solvers.

CaDiCaL times out, our solver solves `6g_6color` within a minute even though it contains 77,328 variables and 8,485,566 clauses. Our solver also solves `Nb13T165` in 22 minutes while handling over one million variables and five million clauses. Considering all 179 satisfiable problems in the Competition, our solver achieves an average total speedup of 27.30x.

Figure 5 demonstrates the cumulative runtime performance on the entire satisfiable problem set. We show the performance curves for our solver along with baselines and variants. We include MiniSat as a reference because it is the foundational SAT solver on which others are developed. We also include Glucose [30] for its different solving heuristics. Each point on a curve denotes the number of problems solved within the given time limit. The plot demonstrates the advantage of our solver over the baselines. Our solver, integrated with either CaDiCaL, Glucose, or MiniSat, solves more problems within shorter time

limits compared to using each respective solver alone. This shows that gradient guidance is effective for different CDCL solvers. In particular, our solver with CaDiCaL achieves the highest performance, solving a total of 165 problems within 5000 seconds. That is 22 more solved than CaDiCaL alone.

Figure 5 also highlights the strength our solver at different time limits. Up to 250 seconds, the curves for our solver climb rapidly regardless of the underlying CDCL solver, indicating that our approach solves problems much more efficiently than baselines. As the time limit increases towards 1000 seconds, the performance gap remains pronounced. Evident in the slopes of the curves, our solver with CaDiCaL outpaces all other methods shown by solving more problems within the same given time. Beyond 2000 seconds, our solver continues to improve while CaDiCaL’s performance plateaus. Overall, our solver with CaDiCaL achieves a PAR2 SAT score [28] of 972.28 compared to 2228.22 for CaDiCaL. We attain this score without clause sharing or other parallel solving techniques.

VI. CONCLUSIONS

The integration of GPU-accelerated gradient-driven optimization with CPU-based conflict-driven search represents a promising frontier for scalable SAT solving. By reformulating SAT as a differentiable binarized matrix multiplication task, our hybrid approach effectively balances the strengths of massively parallel exploration on GPU with targeted sequential search on CPU. By demonstrating its benefits on a commercial GPU-CPU hybrid system, our results highlight the potential of combining modern differentiable optimization with classical search algorithms to overcome inherent parallelism limitations in logical reasoning and combinatorial optimization.

REFERENCES

[1] A. Biere, M. Heule, H. van Maaren, and T. Walsh, eds., *Handbook of Satisfiability*. Frontiers in Artificial Intelligence and Applications, IOS Press, 2021.

[2] J. P. M. Silva and K. A. Sakallah, “GRASP: A Search Algorithm for Propositional Satisfiability,” *Int'l Conf. on Computer-Aided Design (ICCAD)*, 1996.

[3] N. Eén and N. Sörensson, “An Extensible SAT-solver,” *Int'l Conf. on Theory and Applications of Satisfiability Testing (SAT)*, 2003.

[4] A. Biere, T. Faller, K. Fazekas, M. Fleury, N. Froleyks, and F. Pollitt, “CaDiCaL 2.0,” *Int'l Conf. on Computer-Aided Verification (CAV)*, 2024.

[5] V. Ganesh and M. Y. Vardi, “On the Unreasonable Effectiveness of SAT Solvers,” in *Beyond the Worst-Case Analysis of Algorithms*, Cambridge University Press, 2021.

[6] C. Le Frioux, E. Hebrard, B. Mazure, and L. Sais, “Modular and Efficient Divide-and-Conquer SAT Solver on Top of the Painless Framework,” *Int'l Conf. on Tools and Algorithms for the Construction and Analysis of Systems (TACAS)*, 2019.

[7] Y. Hamadi, S. Jabbour, and L. Sais, “ManySAT: A Parallel SAT Solver,” *Int'l Conf. on Theory and Applications of Satisfiability Testing (SAT)*, 2009.

[8] M. Osama, A. Wijs, and A. Biere, “SAT Solving with GPU Accelerated Inprocessing,” *Int'l Conf. on Tools and Algorithms for the Construction and Analysis of Systems (TACAS)*, 2021.

[9] H. Fujii and N. Fujimoto, “GPU Acceleration of BCP Procedure for SAT Algorithms,” *Int'l Conf. on Parallel and Distributed Processing Techniques and Applications (PDPAT)*, 2012.

[10] NVIDIA Corporation, “The NVIDIA Grace Blackwell Superchip.” <https://docs.nvidia.com/multi-node-nvlink-systems/multi-node-tuning-guide/overview.html>.

[11] W. Guo, H.-L. Zhen, X. Li, W. Luo, M. Yuan, Y. Jin, and J. Yan, “Machine Learning Methods in Solving the Boolean Satisfiability Problem,” *Machine Intelligence Research*, 2023.

[12] D. Selsam, M. Lamm, B. Bünz, P. Liang, L. de Moura, and D. L. Dill, “Learning a SAT Solver from Single-Bit Supervision,” *Int'l Conf. on Learning Representations (ICLR)*, 2019.

[13] Z. Shi, M. Li, Y. Liu, S. Khan, J. Huang, H.-L. Zhen, M. Yuan, and Q. Xu, “SATformer: Transformer-Based UNSAT Core Learning,” *Int'l Conf. on Computer-Aided Design (ICCAD)*, 2023.

[14] D. Selsam and N. Bjørner, “Guiding High-Performance SAT Solvers with Unsat-Core Predictions,” *Int'l Conf. on Theory and Applications of Satisfiability Testing (SAT)*, 2019.

[15] W. Wang, Y. Hu, M. Tiwari, S. Khurshid, K. McMillan, and R. Miikkulainen, “NeuroBack: Improving CDCL SAT Solving using Graph Neural Networks,” *Int'l Conf. on Learning Representations (ICLR)*, 2024.

[16] A. Kyriolidis, A. Srivastava, M. Vardi, and Z. Zhang, “FourierSAT: A Fourier-expansion-based algebraic framework for solving hybrid boolean constraints,” *AAAI Conf. on Artificial Intelligence (AAAI)*, 2020.

[17] Y. Cen, Z. Zhang, and X. Fong, “Massively Parallel Continuous Local Search for Hybrid SAT Solving on GPUs,” *AAAI Conf. on Artificial Intelligence (AAAI)*, 2025.

[18] Y. Zhang, H.-L. Zhen, M. Yuan, and B. Yu, “DiffSAT: Differential MaxSAT Layer for SAT Solving,” *Int'l Conf. on Computer-Aided Design (ICCAD)*, 2024.

[19] C. Jajcay and M. Krajecki, “GPU4SAT: Solving the SAT Problem on GPU,” *Conf. on State-of-the-Art in Scientific and Parallel Computing (PARA)*, 2008.

[20] B. Jacob, S. Kligys, B. Chen, M. Zhu, M. Tang, A. Howard, H. Adam, and D. Kalenichenko, “Quantization and Training of Neural Networks for Efficient Integer-Arithmetic-Only Inference,” *Conf. on Computer Vision and Pattern Recognition (CVPR)*, 2018.

[21] P. Yin, J. Lyu, S. Zhang, S. Osher, Y. Qi, and J. Xin, “Understanding Straight-Through Estimator in Training Activation Quantized Neural Nets,” *arXiv preprint arXiv:1903.05662*, 2019.

[22] M. Davis, G. Logemann, and D. Loveland, “A machine program for theorem proving,” *Communications of the ACM*, vol. 5, no. 7, 1962.

[23] C. Ansótegui, M. L. Bonet, and J. Levy, “On the Structure of Industrial SAT Instances,” *Int'l Conf. on Principles and Practice of Constraint Programming*, 2009.

[24] NVIDIA, “NVIDIA DGX GB200: AI Infrastructure for State-of-the-Art AI Models.” <https://www.nvidia.com/en-us/data-center/dgx-gb200/>, 2025.

[25] A. Ignatiev, A. Morgado, and J. Marques-Silva, “PySAT: A Python Toolkit for Prototyping with SAT Oracles,” *Int'l Conf. on Theory and Applications of Satisfiability Testing (SAT)*, 2018.

[26] A. Paszke, S. Gross, F. Massa, A. Lerer, J. Bradbury, G. Chanan, T. Killeen, Z. Lin, N. Gimelshein, L. Antiga, A. Desmaison, A. Kopf, E. Yang, Z. DeVito, M. Raison, A. Tejani, S. Chilamkurthy, B. Steiner, L. Fang, J. Bai, and S. Chintala, “PyTorch: An Imperative Style, High-Performance Deep Learning Library,” *Advances in Neural Information Processing Systems (NeurIPS)*, 2019.

[27] A. Biere, “CaDiCaL SAT Solver, Version 1.9.5.” <https://github.com/arminbiere/cadical>, 2022.

[28] M. J. Heule, M. Iser, M. Järvisalo, and M. Suda, “Proceedings of SAT Competition 2024: Solver, Benchmark and Proof Checker Descriptions,” *Department of Computer Science, University of Helsinki*, 2024.

[29] S. Kirkpatrick and B. Selman, “Critical Behavior in the Satisfiability of Random Boolean Expressions,” *Science*, 1994.

[30] G. Audemard and L. Simon, “Predicting Learnt Clauses Quality in Modern SAT Solvers,” *Int'l Joint Conf. on Artificial Intelligence (IJCAI)*, 2009.